RESEARCH ARTICLE OPEN ACCESS

Elastic Properties of Ho^{3+} Substitution Co-Ferrites Synthesized by Sol-Gel Auto Combustion Method

A. M. Pachpinde*, M.M. Langade*, L.A. Dhale, K.A.Ganure*****

**Departmen of Chemistry, Jawahar ASC College, Anadur, Osmanabad, India*

Email:mallinathlangade@gmail.com

*** (Department of chemistry, Shrikrishna College, Gunjoti, Osmanabad,, India*

**** Department of Nanotechnology, WcRnb, Walchand College, Solapur,, India*

Abstract:

Ho^{3+} doped $Ho_xCoFe_{2-x}O_4$ (x = 0.0, 0.025, 0.05, 0.075, 0.1) ferrite nanoparticles prepared by using sol-gel auto combustion method. The prepared samples sintered at 600 °C for 4 hours. Infrared spectra carried out at room temperature in the wave number range of 300–800 cm^{-1}. The IR spectra show two major absorption bands. High frequency bands 'ν_1' is assigned to the tetrahedral and low frequency bands 'ν_2' is assigned to the octahedral sites of complex. Force constant for the tetrahedral and octahedral site was determined by using IR data. The values of Force constant use to calculate the Stiffness constants (C_{11} and C_{12}). Using the values of stiffness constants; Elastic modulus such as Young's modulus, Rigidity modulus, Poisson's ratio and Debye temperature are calculated.

Keywords — **Sol-gel method, Ferrites, infra- red spectroscopy, Elastic Properties**

I. INTRODUCTION

Spinel nano-ferrites are materials research due to their structural, dielectric, electrical and magnetic properties. [1-2] Co-ferrites are magnetic ferrite with high coercive field and high magneto crystalline anisotropy, and promised wide technological applications [3-5]. Cobalt ferrite has inverse Spinel structure and is of the most versatile Centro symmetric magnetic materials. In the inverse Spinel structure, the tetrahedral [A] sites are occupied by the Fe^{3+} ions, and the octahedral sites (B) are occupied by the divalent metal ions (M^{2+}) and Fe^{3+} in equal proportions. The angle A-O-B is closer to 180° than the angles B-O-B and A-O-A; therefore, the AB pair (Fe-Fe) has a strong super exchange (anti ferromagnetic) interaction [6]. Infrared (IR) spectroscopy is one of the most versatile characterization techniques used to (i) study the occurrence of various absorption bands in the spectrum (ii) determine the local symmetry in crystalline/non-crystalline solids, ordering phenomenon, presence/absence of Jahn–Teller ions (iii) determine force constants, elastic moduli, Debye temperature and molar heat-capacity[7]. The elastic moduli represent the mechanical strength and thermal shock resistance of sample [8]. The nano ferrite $CoHo_xFe_{2-x}O_4$ (x = 0.0, 0.025, 0.05, 0.075, 0.1) were synthesized by Sol-gel Auto-Combustion method and also examine the effect of Ho^{3+} ions substitution in Co-ferrites on the infra-red spectra and study of their elastic properties.

II. EXPERIMENT

The ferrite powders were synthesized through sol-gel auto-combustion route to achieve homogeneous mixing of the chemical constituents on the atomic scale and better sinter ability. AR grade Cobalt Nitrate ($Co(NO_3)_2 \cdot 3H_2O$), Holmium Nitrate ($Ho(NO_3)_3 \cdot 5H_2O$), Iron Nitrate ($Fe(NO_3)_3 \cdot 9H_2O$) and Citric acid ($C_6H_8O_7 \cdot H_2O$), were used to prepare the $HoxCoFe_{2-x}O_4$ (x = 0.0, 0.025, 0.05, 0.075, 0.1) ferrite compositions. Reaction procedure was carried out in air atmosphere without protection of inert gases. The molar ratio of metal nitrates to citric acid was taken as 1:3. The metal nitrates were dissolved together in a minimum amount of double distilled water to get a clear solution. An aqueous solution of citric acid

was mixed with metal nitrates solution, then ammonia solution was slowly added to adjust the pH at 7. Then the solution was heated at 90 ℃ to transform into gel. When ignited at any point of the gel, the dried gel burnt in a self-propagating combustion manner until all gels were completely burnt out to form a fluffy loose powder. The auto-combustion was completed within a minute, yielding the brown-colored ashes termed as a precursor. The as prepared powder then annealed at 600 ℃ for 4 hrs.

Sol-gel auto-combustion synthesized powder samples were the infrared spectra of all the samples were recorded at room temperature in the range 300 cm-1 to 800 cm^{-1} using Perkin Elmer infrared spectrophotometer.

III. RESULT AND DISCUSSION

A. *Infrared spectroscopy*

The room temperature IR spectra of the all the composition are shown in Figure 1. The spectra are recorded in the range from 300 to 800 cm^{-1}. The band positions for all the investigated composition are given in Table 1. The spectra show two main absorption bands 'υ_1' and 'υ_2' as a common feature of all the ferrites. The high-frequency band υ_1 lies in the range 702-725 cm^{-1} while the low-frequency band υ_2 is varying in the 486-497 cm^{-1} range.

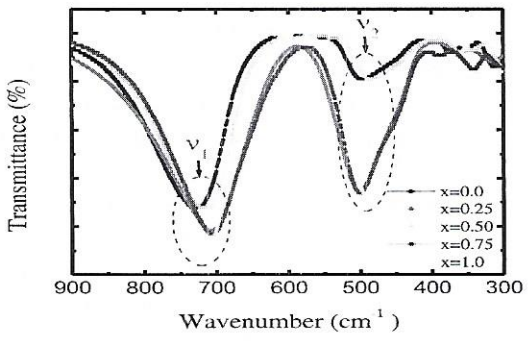

Figure.1. Infrared spectra of $Ho_xCoFe_{2-x}O_4$ (x = 0.0, 0.025, 0.05, 0.075, 0.1)

The difference in the band position is expected because of the difference in Fe^{3+}- O^{2-} distance for the octahedral and tetrahedral compounds. From the IR spectra it is noticed that the frequency 'υ_1' and 'υ_2' are slightly shifted with an increasing Ho^{3+} concentration and consequently with decreasing Fe ions concentration. Waldron [9] studied the vibration spectra of ferrites and attributed the $\upsilon 1$ band to the intrinsic vibrations of the tetrahedral groups and 'υ_2' band to the octahedral groups. Thus, the replacement of Ho^{3+} with Fe^{3+} ions (having larger ionic radius and higher atomic weight than Fe^{3+}) at octahedral site in the ferrite lattice affects the Fe^{3+}- O^{2-} stretching vibration. This may be reason for the observed change in $\upsilon_1$and υ_2 band positions [10].

According to Waldron the force constant K_t and K_0 for respective sites are given by:

$$K_t = 7.62 \times M_1 \times \nu_1^2 \times 10^{-3} \quad (1)$$

$$K_0 = 10.62 \times \frac{M_2}{2} \times \nu_2^2 \times 10^{-3} \quad (2)$$

Where, K_0 = force constant on octahedral site,

K_t = force constant on tetrahedral site,

M_1=Molecular weight of tetrahedral site,

M_2=Molecular weight of octahedral site,

ν_1=Corresponding frequency on tetrahedral site,

ν_2= Corresponding frequency on octahedral site.

TABLE 1.

LATTICE CONSTANT (a), X-RAY DENSITY (dx), BAND POSITION ($\nu_1$and ν_2), FORCE CONSTANT (K_0 and K_t) $Ho_xCoFe_{2-x}O_4$

Comp. x	'a' (Å)	'dx' (g/cm³)	Band position		Force constant	
			ν_1 (cm^{-1})	ν_2 (cm^{-1})	$K_0 \times 10^5$ (dyne/cm)	$K_t \times 10^5$ (dyne/cm)
0.00	8.355	5.345	725	497	1.550	2.239
0.025	8.363	5.392	708	499	1.490	2.115
0.05	8.373	5.436	714	491	1.376	2.123
0.075	8.379	5.484	702	496	1.326	2.053
0.10	8.383	5.536	725	486	1.186	2.030

The values of force are summarized in above Table 1. The force constant K_t decreasing with the increasing Ho^{3+} content whereas K_0 decreases with the increasing in Ho^{3+}. This variation can be related with the difference in ionic radii of Fe^{3+} and Ho^{3+} ions and their occupancy at A and B sites. Analysis of IR spectra with crystallographic knowledge helps us to determine the Debye temperature and elastic properties. The Debye temperature (θ_I) of all samples was calculated using the wave number of IR bands [9].

$$\theta l = hCVac/k \quad (3)$$

Where, h = h/2π,

k = Boltzman constant,

C = velocity of light ($3x10^8$ cm/s)

V_{ac} = average wave number of bands

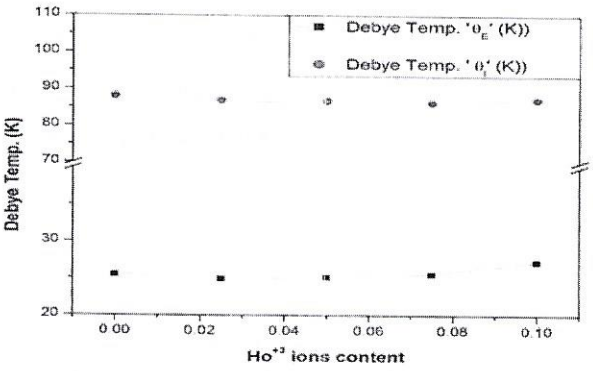

Figure 2.Variation of Debye temperature calculated form infrared (θ_I) and elastic (θ_E) with Ho^{3+} content

B. Elastic properties

The elastic properties were determined using infrared spectroscopy [11-12] These elastic moduli were calculated using the values of lattice constant 'a', X-ray density 'dx', pore fraction 'f' and force constant 'K'. Values of lattice constant, X-ray density and pore fraction are listed in Table 1. The average force constant (K) was calculated using the following relation:

$$K=K_t+K_0/2 \quad (4)$$

The bulk modulus of term stiffness constant C_{11} was calculated using relation [13]

Stiffness constant

$$C_{11} = \frac{K}{a} \quad (5)$$

Where, K is average force constant and 'a' is lattice constant.

Stiffness constant

$$(C_{12}) = \frac{\sigma \times C_{11}}{(1-\sigma)} \quad (6)$$

Where, 'σ' is Poisson ratio and 'a' is the lattice constant.

The Poisson ratio is function of pore fraction (σ = 0.324 x 1 -1.043f). Values of Poisson ratio are described in Table 2. The Poisson ratio is ranges in between 0.276 and 0.266; these values are lying in the range of -1 to 0.5, which is in conformity with the theory of isotropic elasticity. [12].

Variation of stiffness constants (C_{11} and C_{12}) as a function of Ho^{3+} content is shown in Table 2. It is observed from Table 2; both the stiffness constant was decreases with increase in Ho^{3+} substitution.

TABLE 2

MEAN FORCE CONSTANT (K), PORE FRACTION STIFFNESS CONSTANT (C_{11} and C_{12}), of $Ho_xCoFe_{2-x}O_4$.

Comp. x	Mean Force constant (K) (K_t+K_0)	Pore Fraction	Passion's ratio σ	C_{11}	C_{12}
0.00	1.8943	0.141	0.276	226.73	86.58
0.025	1.88029	0.147	0.274	215.58	81.50
0.05	1.7498	0.154	0.272	209.01	78.07
0.075	1.6899	0.160	0.269	201.68	74.57
0.10	1.7080	0.168	0.266	203.75	74.30

The values of Poisson's ratio were calculated using the relation discussed elsewhere [14] and the values are presented in Table 2.Stiffness constant are affected by two factors; i.e. the tightness of bonding between the atoms and force constant. In present system bonds between Fe^{3+} and Ho^{3+} atoms is residual bond and due to this stiffness constant are decreases with increasing

Ho content. These two stiffness constants are further used to calculate the various elastic constants such as; Young's modulus (E), bulk modulus (K) and modulus of rigidity (G) [14]. The other elastic moduli for cubic structure are calculated using following relation [15].

$$\text{Rigidity modulus } (G) = \frac{E}{2(\sigma+1)} \qquad (7)$$

The rigidity modulus (G) is calculated using the relation 7 and the variation are presented in Figure 3 as shown below.

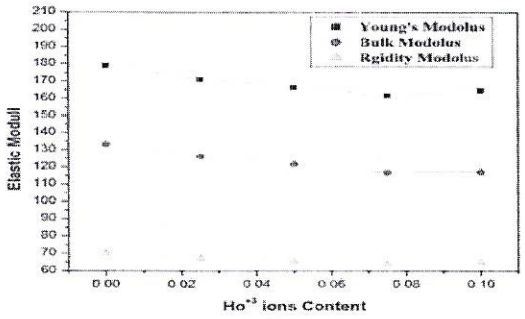

Figure 3.Variation of Young's modulus (E), bulk modulus (K) and modulus of rigidity (G) with Ho^{3+} content.

Young's modulus (E), bulk modulus (K) and modulus of rigidity (G) decrease with increase in both Ho^{3+}. It indicates that deformation of the solid is easy and the solid has fewer tendencies to spring back to its equilibrium position. The Young's modulus, Bulk modulus and Modulus of rigidity decrease with the increasing Ho^{3+} content. The decreases in elastic moduli may be due to the interatomic binding between various atoms in the spinel lattice [15]. The inter-atomic bonding between the various atoms weakens continuously with the addition of Ho^{3+} content and therefore elastic moduli decreases with the increasing Ho^{3+}content. In Fe^{3+}-Ho^{3+} ferrite repulsion between electrons may be increased with the increasing Ho^{3+} content [16].

The longitudinal elastic wave velocity (V_L) and transverse (Shear) wave velocity (V_S) were calculated using following equations.

$$\text{Longitudinal velocity } V_L = \left(\frac{C_{11}}{\rho}\right)^{1/2} \qquad (8)$$

Transverse (Shear) velocity

$$V_S = \left(\frac{G}{\rho}\right)^{1/2} \qquad (9)$$

Where, G is rigidity modulus with correct zero pore fraction. The values of V_l and V_s used to calculate mean wave velocity (V_m) which used to calculate Debye temperature was calculated using formula.

Debye temperature

$$\theta_E = \frac{h}{k}\left[\frac{3\rho q N_A}{4\Pi M}\right]^{1/3} \times V_m \qquad (10)$$

Where, h is planks constant, k is Boltzmann's constant, M is molecular weight, q is number if atom in the unit formula and V_m mean wave velocity.

$$\frac{3}{V_m^3} = \frac{1}{V_l^3} + \frac{2}{V_s^3} \qquad (11)$$

The values of longitudinal wave, shearing wave and mean wave velocity are calculated using relation 8, 9 and 10 respectively. It is observed shown in Figure 4 the longitudinal elastic wave velocity is decreases whereas transverse (Shear) wave velocity increased with Ho^{3+} substitution.

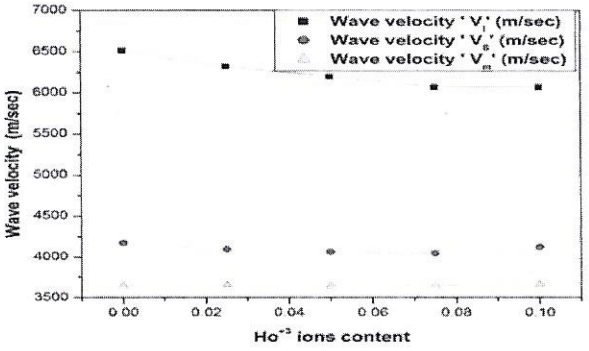

Figure 4.Variation of shearing velocity (V_S), mean wave velocity (V_m) and longitudinal wave velocity (V_L) with Ho^{3+}content.

The values of wave velocities are similar to other ferrites those obtained from UPT method [17]. The variation of Debye temperature (θ_E) is shown in the Figure 2. The Debye temperature increased with Ho^{3+} substitution. It suggested that lattice vibrations are hindered due to Ho^{3+}substitution. This may be due to the fact that strength of interatomic bonding increases with concentration (x and y) as supported by our results on the variation of elastic moduli [18].

The variation of Debye temperature (θ_E) calculated by using the relation 12. Given in Figure.2. The values of V_l/p and V_S/p are calculated by Anderson equation [19] shown in Figure .5. This behaviour clearly indicates the direct relationship between the acoustic parameter (average sound velocity) and the important thermodynamic parameter Debye temperature [20].

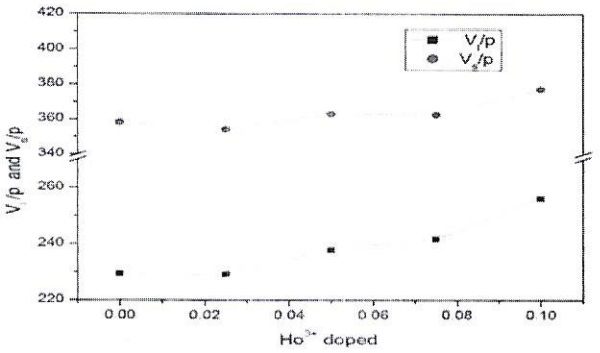

Figure 5.V_l /p and V_s/p against Ho^{3+} ion content.

IV. CONCLUSIONS

The Ho^{3+} substituted Co ferrite nanoparticles were prepared by using the sol-gel auto-combustion method. IR spectra confirmed the formation of Spinel structure and gave information about the distribution of ions between the two sites, tetrahedral (A-site) at 702-725 cm^{-1} and octahedral (B-site) at 486-497 cm^{-1}. The Elastic properties such as elastic wave velocity, elastic constant and Debye temperature calculated using IR data. The elastic constants decreased with the increase in Ho^{3+} content. The elastic moduli decreasing with increasing Ho^{3+} content and Debye Temperature are found to increasing with increasing Ho^{3+} content.

REFERENCES

[1] Lodhi, M. Y., Mahmood, K., Mahmood, A., Malik, H., Warsi, M. F., Shakir, I & Khan, M. A. (2014). New Mg0. 5CoxZn0. 5−xFe2O4 nano-ferrites: structural elucidation and electromagnetic behavior evaluation. *Current Applied Physics*, *14*(5), 716-720

[2] Lee, S. W., Bae, S., Takemura, Y., Shim, I. B., Kim, T. M., Kim, J & Kim, C. S. (2007). Self-heating characteristics of cobalt ferrite nanoparticles for hyperthermia application. Journal of Magnetism and Magnetic Materials, 310(2), 2868-2870.

[3] Martens, J., & Voermans, A. (1984). Cobalt ferrite thin films for magneto-optical recording. IEEE Transactions on Magnetics, 20(5), 1007-1012.

[4] Abe, M., Itoh, T., & Tamaura, Y. (1992). Magnetic and biomagnetic films obtained by ferrite plating in aqueous solution. *Thin Solid Films*, *216*(1), 155-161.

[5] Tamaura, Y., Kojima, M., Hasegawa, N., Tsuji, M., Ehrensberger, K., & Steinfeld, A. (1997). Solar energy conversion into H2 energy using ferrites. *Le Journal de Physique IV*, *7*(C1), C1-673.

[6] Sivakumar, N., Narayanasamy, A., Chinnasamy, C. N., & Jeyadevan, B. (2007). Influence of thermal annealing on the dielectric properties and electrical relaxation behaviour in nanostructured CoFe2O4 ferrite. *Journal of Physics: Condensed Matter*, *19*(38), 386201

[7] Zaki, H. M., & Dawoud, H. A. (2010). Far-infrared spectra for copper–zinc mixed ferrites. *Physica B: Condensed Matter*, *405*(21), 4476-4479.

[8] Patange, S. M., Shirsath, S. E., Jadhav, S. P., Hogade, V. S., Kamble, S. R., & Jadhav, K. M. (2013). Elastic properties of nanocrystalline aluminum substituted nickel ferrites prepared by co-precipitation method. *Journal of Molecular Structure*, *1038*, 40-44.

[9] Waldron, R. D. (1955). Infrared spectra of ferrites. *Physical review*, *99*(6), 1727

[10] Lohar, K. S., Pachpinde, A. M., Langade, M. M., Kadam, R. H., & Shirsath, S. E. (2014). Self-propagating high-temperature synthesis, structural morphology and magnetic interactions in rare-earth Ho^{3+} doped $CoFe_2O_4$ nanoparticles. *Journal of Alloys and Compounds*, *604*, 204-210.

[11] Modi, K. B., Gajera, J. D., Pandya, M. P., Vora, G., & Joshi, H. H. (2004). Far-infrared spectral studies of magnesium and aluminum co-substituted lithium ferrites. Pramana, 62(5), 1173-1180.

[12] "Variation in Elastic Properties of Holmium substituted Nickel Copper Zinc Ferrites". B. L Shinde, L. A. Dhale, K. A Ganure, K. S.Lohar. *Asian Journal of Chemistry, 2017, 29(11), pp. 2531-2535.*

[13] Kakani, S. L., &Hemrajani, C. (1997). Textbook of solid-state physics. Sultan Chand & Sons, New Delhi.

[14] Pathak, T. K., Buch, J. J. U., Trivedi, U. N., Joshi, H. H., & Modi, K. B. (2008). Infrared co-precipitation technique. *Journal of nanoscience and nanotechnology*, *8*(8), 4181-4187

[15] Infrared spectroscopy and elastic properties of copper substituted nickel zinc ferrite" U.M. Mandle, L.A. Dhale, Ketan A. Ganure, B.L. Shinde and K.S. Lohar., *Asian Journal of Chemistry, 2019 ,31(2), pp. 367-372.*

[16] IR Spectral and Elastic Moduli study of Ho^{+3} doped Co–Ni ferrites via Sol–gel auto combustion Method". Fugate D V. Ganure Ketankumar A, Dhale Laxaman A, Kadam Ankush. B. *Int. Res. J. of Science & Engineering, 2018 9(2), pp.1-6.*

[17] Wooster, W. A. (1953). Physical properties and atomic arrangements in crystals. *Reports on Progress in Physics*, *16*(1), 62.

[18] Mazen, S. A., &Elmosalami, T. A. (2012). Structural and elastic properties of Li-Ni ferrite. ISRN Condensed Matter Physics, 2011

[19] Anderson, O. L., Mason, W. P., & Thurston, R. N. (1965). Physical Acoustics. Vol. III, Part B.

[20] Revathi, M. B., & Rao, T. S. (1974). Elastic behavior of mixed cobalt-zinc ferrites. *Journal of the Less-Common Metals*, *34*(1), 91-96.